

Session 01C02

Droplet and Particle Formation in the Electrohydrodynamic Atomization

Liang Kuang Lim¹, Jingwei Xie², Jinsong Hua³, Chi-Hwa Wang^{1,2},
Kenneth A. Smith^{1,5}.

¹ MEBCS Program, Singapore-MIT Alliance, 4 Engineering Drive 3, 117576, Singapore, Singapore

² Department of Chemical and Biomolecular Engineering, National University of Singapore, 4 Engineering Drive 4, Singapore, 117576, Singapore

³ Institute of High Performance Computing, 1 Science Park Road #01-01 The Capricorn, Singapore Science Park II, Singapore 117528

⁴ National University of Singapore, Department of Chemical and Biomolecular Engineering, Singapore, 117576, Singapore

⁵ Department of Chemical Engineering, Massachusetts Institute of Technology, Cambridge, MA 02139

Introduction

Electrohydrodynamic atomization (EHDA) has been studied and documented for over a century^{1,2,3,4}. In recent years, there is a renewed interest in harnessing its ability to produce monodisperse liquid droplets for the fabrication of monodisperse polymeric particles^{5,6,7}. In this method, a solution of organic solvent and polymeric solute is sprayed using EHDA. An electrical potential is applied to the nozzle which is countered by a grounded copper plate placed below. This leads to the formation of a liquid cone at the tip of the nozzle, which is termed the Taylor Cone. A very fine jet is formed at the tip of the Taylor Cone. This jet then breaks up to produce a cloud of monodisperse droplets. The organic solvent will then evaporate from the surface of the droplets, leaving behind solid polymeric particles (Figure 1).

To produce particles of controllable size, it is important to understand the effects of the various fabrication parameters, such as electrical field strength, surface charge density and solution flow rate, on both the jet diameter and the final droplet size. Hence, computational fluid dynamics (CFD) was used to simulate the formation of the Taylor Cone and jet in a geometry similar to the actual laboratory facility. Encouraging preliminary results have been obtained, with trends showing how the electrical field strength affects the formation of the Taylor Cone and jet, and the effect on the diameter of the droplets obtained during the EHDA process.

Computational Fluid Dynamics

Previously, Hohman⁸ and Hartman⁹ used a one dimensional model to simulate the Taylor Cone and Jet. Unfortunately, their models were unable to capture the droplet formation process. In this study, to simulate the formation of the Taylor Cone and jet, and the breakup of the liquid jet, a computational simulation based on a Front Tracking/Finite Difference model¹⁰ was used. This model has been successfully deployed to simulate the formation of bubble in liquids¹¹ in our previous work. In the case of EHDA, electrical stresses must be taken into account. To define the electrical stress, the divergence of the Maxwell Stress Tensor was taken¹² to give the electrical stress which, in the incompressibility limit, gives:

$$\nabla \cdot \sigma^M = -\frac{1}{2} \bar{E} \cdot \bar{E} \nabla \varepsilon + \rho^f \bar{E} \quad (1.)$$

where \bar{E} is the vector electrical field, ε is the electrical permittivity and ρ^f is the space charge density. This electrical stress term is included in the conservation of fluid momentum equation and acts as a body force. The modified version of the conservation of fluid momentum equation is:

$$\frac{\partial \rho \bar{u}}{\partial t} + \nabla \cdot \rho \bar{u} \bar{u} = -\nabla p + \nabla [\mu (\nabla \bar{u} + \nabla \bar{u}^T)] + \sigma \bar{\kappa} \bar{n} \delta(\bar{x} - \bar{x}_f) + (\rho - \rho_g) \bar{g} - \frac{1}{2} \bar{E} \cdot \bar{E} \nabla \varepsilon + \rho^f \bar{E} \quad (2.)$$

where ρ is the density, \bar{u} is the velocity vector, p is the pressure, μ is the viscosity, σ is the surface tension, κ is the surface curvature, \bar{n} is the unit surface normal vector, ρ_g is the density of the gas phase and \bar{g} is the gravitational constant. $\delta(\bar{x} - \bar{x}_f)$ is a function for which the value is 1 at the interface and 0 everywhere else. This is used to impose the surface tension force at the grid points where the interface lies. This modified conservation of fluid momentum equation is then solved for the whole domain (including the liquid and gas phase) and the interface is tracked.

Due to the complicated nature of the simulated system, the electrical potential field predicted by the Poisson's equation together with the exact boundary conditions is simulated using Domain A and subsequently superimposed on a much smaller geometrical Domain B near the tip of the nozzle. A constant electrical charge density is imposed at the liquid-air interface as a form of user input. The value of the electrical charge density at the liquid-air interface is selected by comparing the simulated Taylor Cone and jet profile to high resolution still shot of actual experiments. Using the above assumptions and simplifications, a reasonable depiction of the EHDA Taylor Cone and jet was achieved (Figure 2).

Taylor Cone and Jet

When the ring electrical potential is varied, the cone angle of the Taylor Cone (Figure 3) also varies. Although there are changes in the cone angle, the jet from the Taylor Cone remains stable. By increasing the ring electrical potential, there

is a gradual reduction of the cone angle of the Taylor cone, which is qualitatively similar to the experimental data. The difference between the experimental cone angle and the prediction can likely be attributed to the constant interface charge density used in this set of simulations.

The changes of the ring electrical potential also cause a change in the diameter of the EHDA jet (Figure 4). Increasing the ring electrical potential may increase the diameter of the jet. This suggests that the ring electrical potential can be used for fine control of the fiber diameters formed by electrospinning¹³.

Droplet Size

Finally, the droplet size obtained from the EHDA system is calculated through the simulation data (Figure 5). Figure 6 shows that changes in the ring electrical potential can cause a change in the diameter of the droplets. It was observed that the predicted changes in the simulated droplet size are similar to that observed in experimental measurements obtained with a Phase Doppler Particle Analyzer. The difference between the experimentally determined droplet size and the predicted size can likely be attributed to the use of a constant interfacial charge density.

Conclusion

We have successfully recreated the EHDA Taylor Cone and Jet by using computational fluid dynamic simulations with a Front Tracking/Finite Difference scheme. The preliminary simulations of the Taylor Cone and Jet depicted the EHDA process reasonably. The effect of ring electrical potential on the Taylor Cone, Jet and droplet formation has been analyzed through simulation, and the trends are consistent with our experimental data. Deviations between the simulations and the experimental data can probably be attributed to the use of a constant interfacial charge density. A more rigorous model for the interface charge density is to be developed.

Acknowledgement

This work is supported by Agency for Science Technology and Research (A*STAR) and National University of Singapore (NUS) under the grant number R279-000-208-305.

References

¹ Basset, A. B., Waves and jet in a viscous liquid, *American Journal of Mathematics*, **16**, 93-110, 1894

- ² Zeleny, J., Instability of electrified liquid surfaces, *Physical Review*, **10**, 1-6, 1917
- ³ Vonnegut, B., Neubauer, R. L., Production of monodisperse liquid particles by electrical atomization, *Journal of Colloidal Science*, **7**, 616-622, 1952
- ⁴ Magaver, R. H., Outhouse, L. E., Note on the break-up of a charged liquid jet, *Journal of Fluid Mechanics*, **13**, 151-157, 1962
- ⁵ Ding, L., Lee, T., Wang, C. H., Fabrication of Monodispersed Taxol Loaded Particles using Electrohydrodynamic Atomization, *Journal of Controlled Release*, **102**, 395-413, 2005.
- ⁶ Xie, J. W., Marijnissen, J. C. M., Wang, C. H., Microparticles Developed by Electrohydrodynamic Atomization for the Local Delivery of Anticancer Drug to treat C6 Glioma In Vitro, *Biomaterials*, **27**, 3321-3332, 2006.
- ⁷ Xie, J. W., Lim, L. K., Phua, Y. Y., Hua, J. S., Wang, C. H., Electrohydrodynamic atomization for biodegradable polymeric particle production, *Journal of Colloid and Interface Science*, **302**, 103-112, 2006.
- ⁸ Hohman, M. M., et. al., Electrospinning and electrically forced jets. II. Applications, *Physics of Fluid*, **12**, 2221-2236, 2001.
- ⁹ Hartman, R. P. A., et. al., Electrohydrodynamic Atomization in the Cone-Jet Mode Physical Modelling of the Liquid Cone and Jet, *Journal of Aerosol Science*, **30**, 823-849, 1999.
- ¹⁰ Trygvason, G., Bunner, B., Esmaeeli, A., Juric, D., Al-Rawahi, N., Tauber, W., Han, J., Nas, S., Jan, Y.-J., A Front Tracking Method for Computations of Multiphase Flow, *Journal of Computational Physics*, **169**, 708-759, 2001.
- ¹¹ Hua, J.S., et. al., Simulation of Bubble Rise and Deformation in Liquid Using A Front Tracking/ Finite Difference Method, *Computational Technologies for Fluid/Thermal/Structure/Chemical Systems with Industrial Applications*, **2**, 225-234, 2001.
- ¹² Saville, D. A., Electrohydrodynamics: The Taylor-Melcher Leaky Dielectric Model, *Annual review of Fluid Mechanics*, **29**, 26-64, 1997.
- ¹³ Xie, J. W., Wang, C. H., Electrospun Micro- and Nanofibers for Sustained Delivery of Paclitaxel to Treat C6 Glioma in Vitro, *Pharmaceutical Research*, **23**, 1817-1826, 2006.

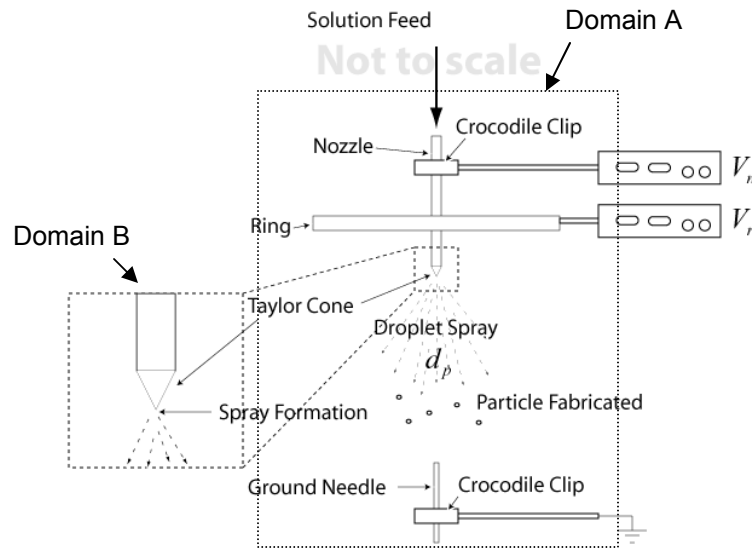


Figure 1: Geometry of the EHDA system. The nozzle electrical potential, V_n , is kept constant at 8kV but the ring electrical potential, V_r , is varied. Domain A is used for the simulation of the electrical potential field. Domain B uses the electrical potential field calculated in Domain A for the CFD simulation. d_p is the measured diameter of the droplets

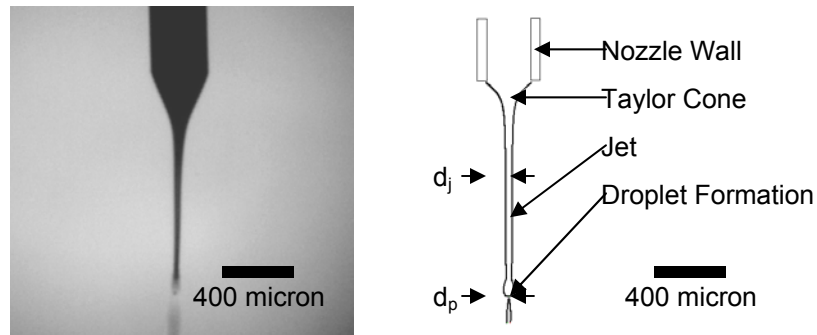


Figure 2: (Left) Backlit photo of the EHDA Taylor Cone and Jet. (Right) Simulated Taylor Cone and Jet. The solution used is dichloromethane at a flow rate of 6 ml/h. The estimated value of the interfacial charge density of $3.6 \times 10^{-5} \text{ C/m}^3$. d_j is the measured diameter of the jet, while d_p is the measured diameter of the droplets.

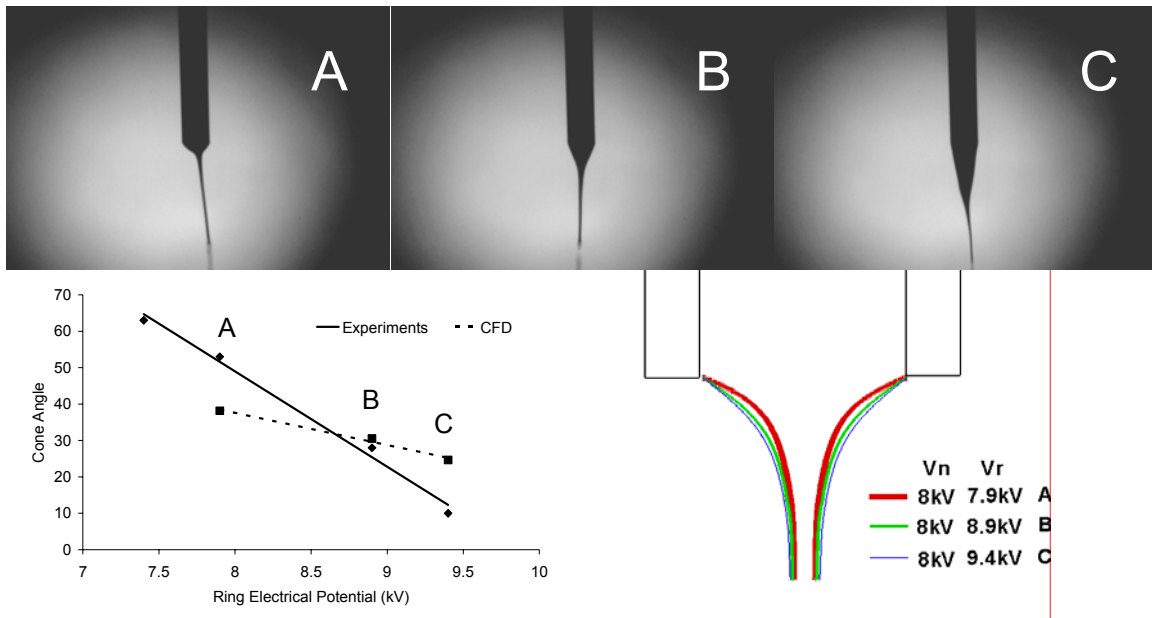


Figure 3: Changes in the cone angle when the ring electrical potential is increased. A similar trend is observed in the experimental data and in the simulation. A, B, C represent corresponding ring electrical potentials in both the experiments and the simulations. The liquid used is dichloromethane at a flow rate of 6ml/h. The estimated interfacial charge density is $3.6 \times 10^{-5} \text{ C/m}^3$. (Top) Photographs of Taylor Cone. (Bottom left) Comparison of experimental and simulation data. (Bottom Right) Simulated Taylor Cone.

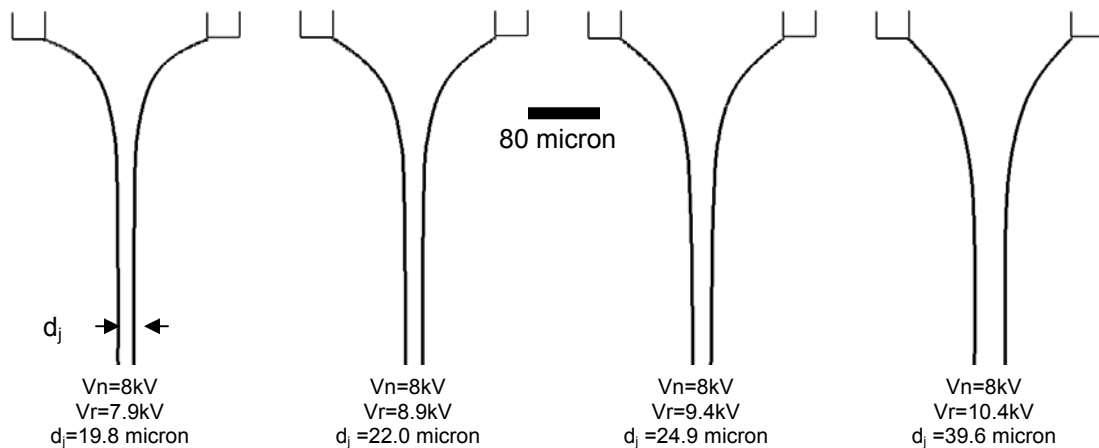


Figure 4: Changes in the jet diameter as the ring electrical potential is increased. The liquid used is dichloromethane at a flow rate of 6ml/h. The estimated interfacial charge density $3.6 \times 10^{-5} \text{ C/m}^3$. d_j represents the measured diameter of the jet

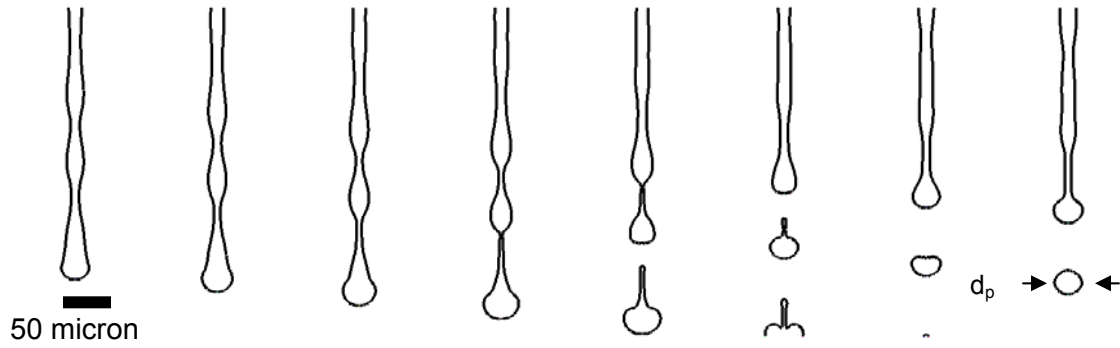


Figure 5: Unstable wave-like structure at the end of the liquid jet before pinch-off to form droplets. Left to right: the evolution of droplet formation from jet. The interval between each frame is 12 microseconds. The liquid used is dichloromethane at a flow rate of 6ml/h. The selected value of the interfacial charge density is $3.6 \times 10^{-5} \text{ C/m}^3$. d_p represents the measured diameter of the droplets

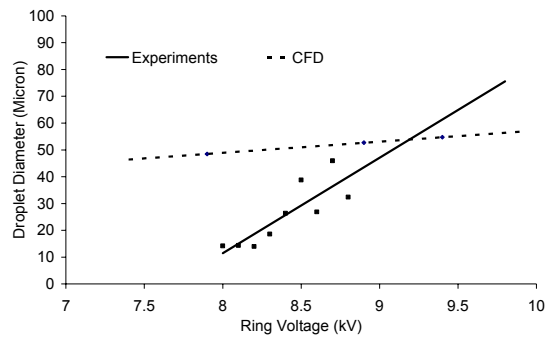


Figure 6: Changes in the droplet size when the ring electrical potential is changed. Both simulation and experimental data are presented. The liquid used is dichloromethane at a flow rate of 6ml/h. The selected value of the interfacial charge density is $3.6 \times 10^{-5} \text{ C/m}^3$.